

“Granular metals and superconductors”

M. V. Feigel'man (L.D.Landau Institute, Moscow)

ICTS Condensed matter theory school, Mahabaleshwar, India, Dec.2009

Lecture 1. Disordered metals: quantum corrections and scaling theory.

Lecture 2. Granular metals

Lecture 3. Granular superconductors and Josephson Junction arrays

Lecture 4. Homogeneously disordered SC films and S-N arrays

Lecture 5. Superconductivity in amorphous poor conductors:

Lecture 1.

Disordered metals: quantum corrections and scaling theory

Plan of the Lecture

- 1) Dimensionless conductance and its scaling
- 2) Interference corrections to conductivity and magnetoresistance
- 3) Spin-orbit scattering and “anti-localization”
- 4) Aronov-Altshuler corrections due to e-e interaction
- 5) Fractal nature of critical wave-functions: is simple scaling valid ?

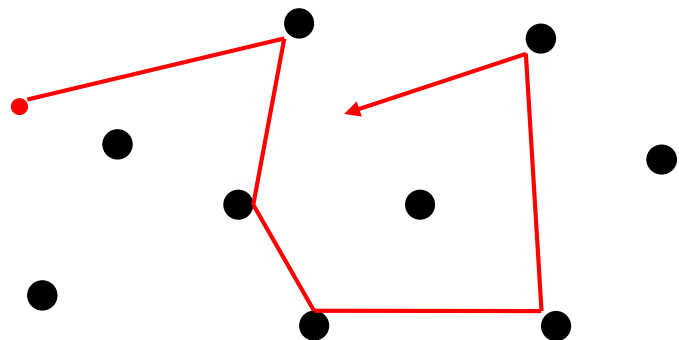
Classical Reviews:

Lee and Ramakrishnan: Disordered electronic systems Reviews of Modern Physics, Vol. 57, No. 2, April 1985

Altshuler, B. L., and A. G. Aronov, 1984, in *Electron-Electron Interactions in Disordered Systems*, edited by M. Pollak and A.

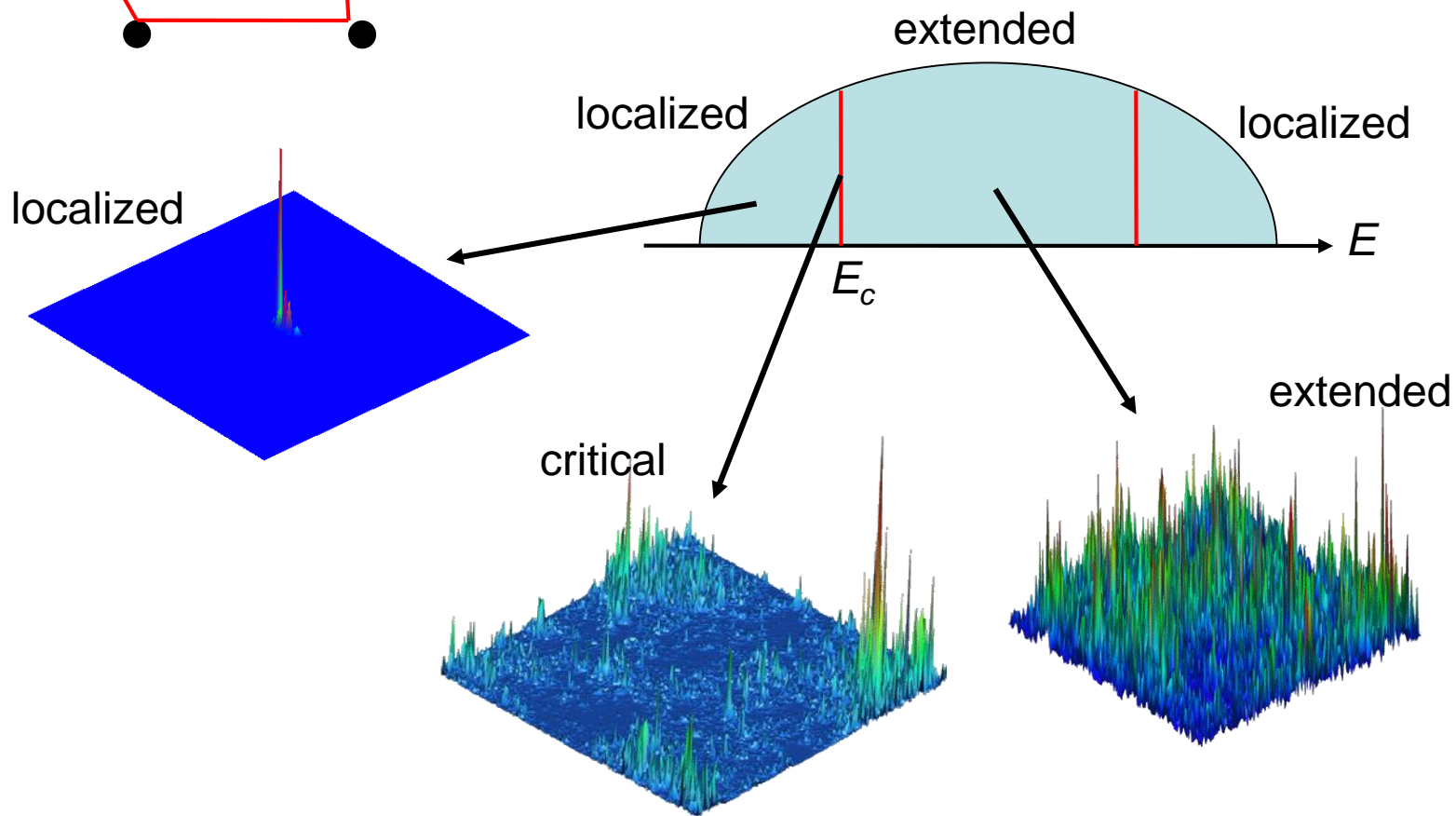
A.M. Finkel'stein, Sov. Sci. Rev. A Phys. 14 (1990) 1.

A non-interacting electron moving in random potential



Quantum interference of scattering waves

→ Anderson localization of electrons



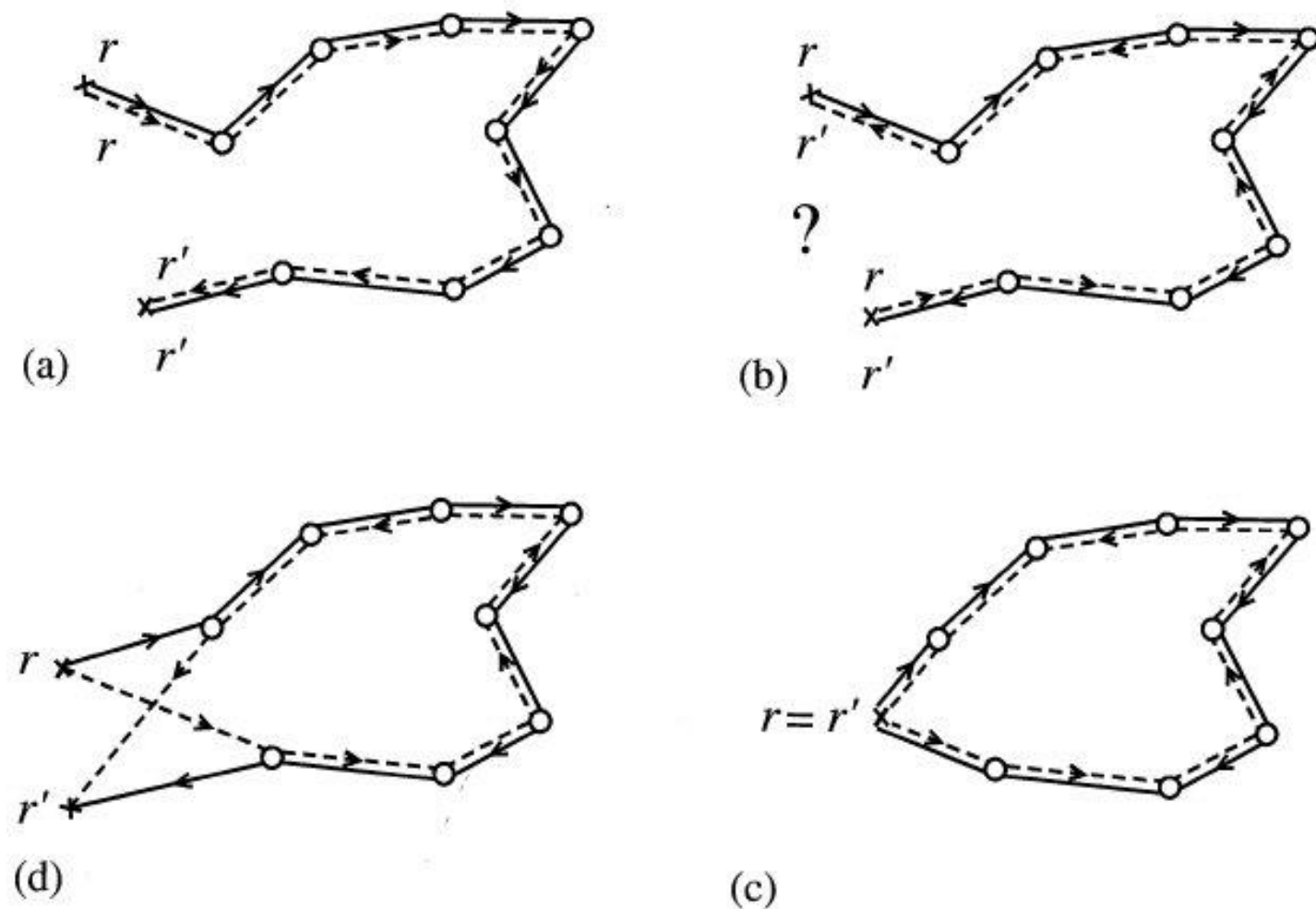


Figure 4.7 (a) Diffuson contribution to the probability. (b) Reversing one of the two trajectories, the points r and r' are exchanged, leading to an impossibility unlike r and r' coincide. In such a case (c), the phases cancel in this new contribution. (d) If $r \neq r'$, there is a mismatch between the two trajectories, leading to a phase shift.

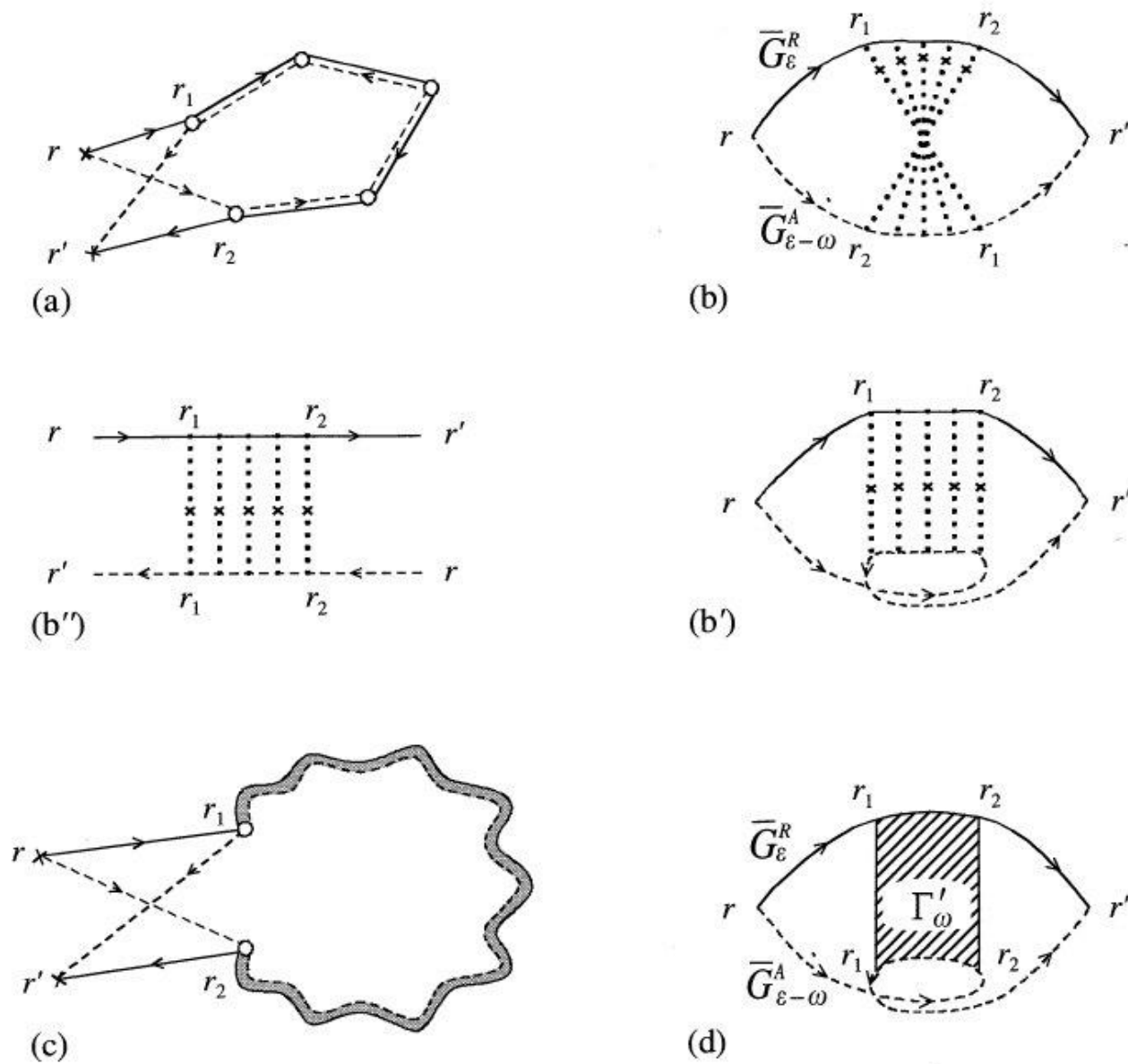
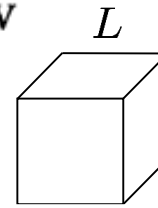


Figure 4.8 (a, b, b', b'') Several equivalent representations of a process of five collisions which contribute to X_c . Representation (b) is common in the literature, and is called a Cooperon or *maximally crossed diagram*. Reversing one of the two trajectories ($b \rightarrow b' \rightarrow b''$), we see that the Cooperon has a ladder structure very similar to that of the Diffuson. (c,d) Representations of X_c . These two figures should be compared with Figures 4.4(c,d) and demonstrate why the Cooperon is a short range



Scaling theory (“gang of four”, 1979)

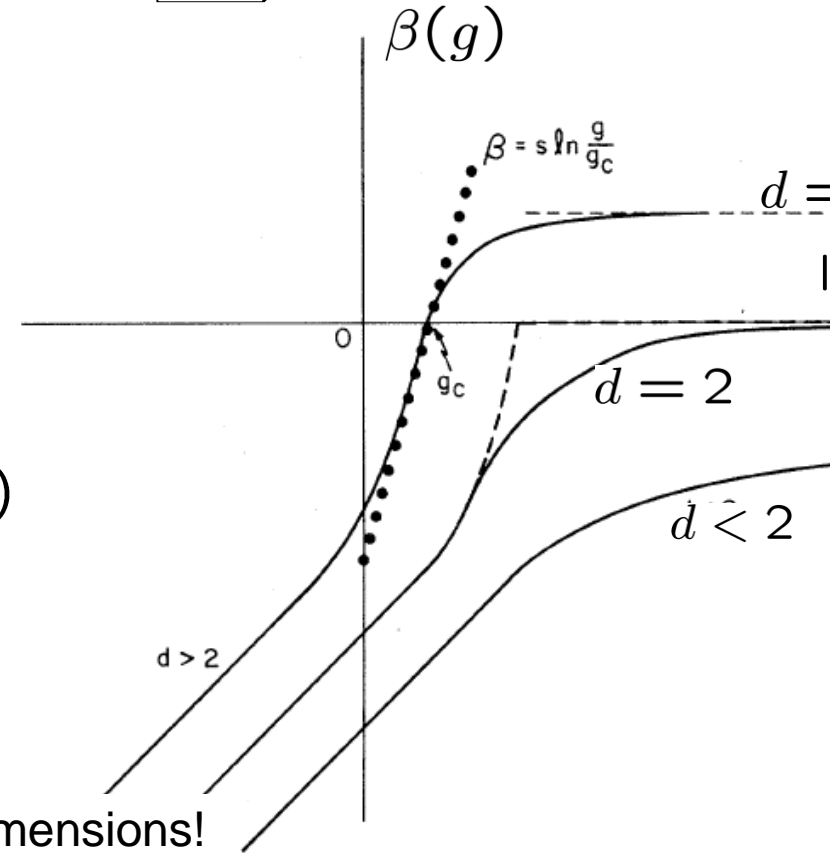
Conductance g changes when system size L changes.

Metal: $g \propto \frac{\text{area}}{\text{length}} = L^{d-2}$

Insulator: $g \propto e^{-L/\xi}$

$$\beta(g) = \frac{d \ln g}{d \ln L} = d - 2 - \mathcal{O}(g^{-1})$$

$g \gg 1$

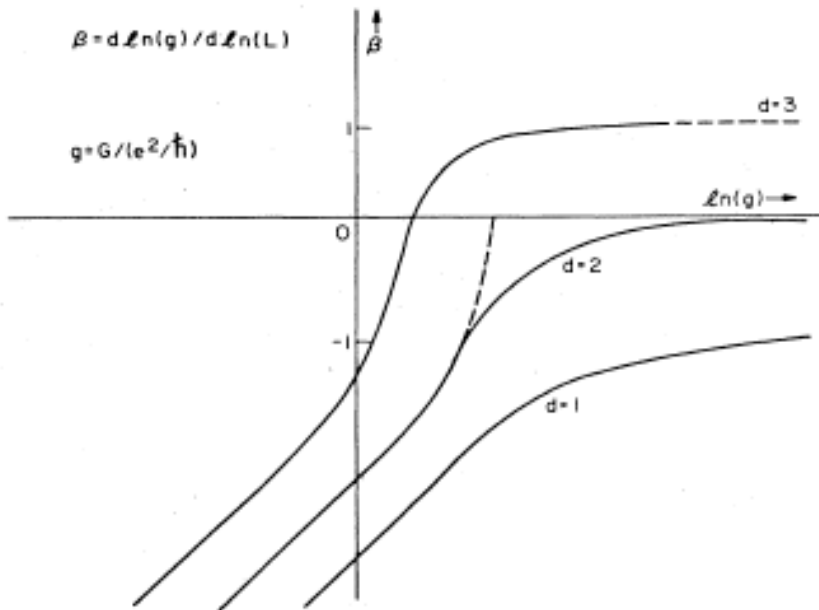


All wave functions are localized below **two** dimensions!

A metal-insulator transition at $g=g_c$ is **continuous** ($d>2$).

$$g(L) = \text{const } L^{d-2}$$

Classical (Drude) conductivity



$$d \ln g / d \ln L = \beta(g)$$

$$\begin{aligned} \beta(g) &= (d-2) - 1/g && \text{at } g \gg 1 \\ &= \ln g && \text{at } g \ll 1 \end{aligned}$$

This is for scattering on purely potential disorder

For strong Spin-Orbit scattering $(-1/g) \rightarrow (+1/2g)$

“Anti-localization” due to S-O

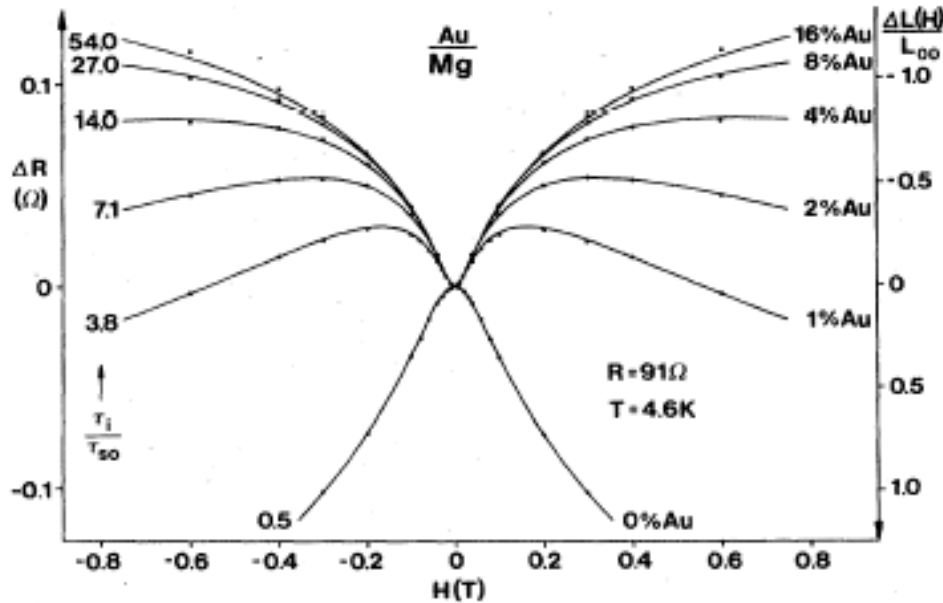
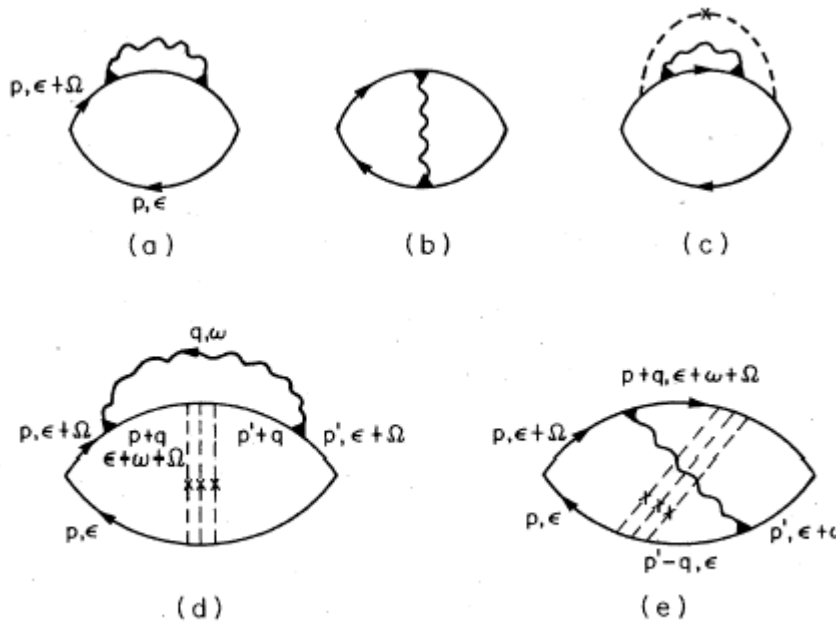


FIG. 17. The magnetoconductance curve of a Mg film with different coverages of Au. [$\Delta L(H)$ is the magnetoconductance, and $L_{\infty} = e^2/2\pi^2\hbar$.] The coverages shown are in percent of an atomic layer. Increasing Au coverage converts the positive magnetoconductance to negative. Full curves through the data points are fits using the theory of Hikami, Larkin, and Nagaoka (1980). Figure is taken from Bergmann (1982b).

e-e interaction corrections (Altshuler & Aronov)



$$\delta\sigma_1 = -\frac{1}{A} \frac{e^2}{\hbar} \frac{1}{2\pi} \left(4 - \frac{3}{2} \tilde{F}_\sigma\right) (D/2T)^{1/2}$$

for 1D,

$$\delta\sigma_1 = \frac{e^2}{\hbar} \frac{1}{4\pi^2} \left(2 - \frac{3}{2} \tilde{F}_\sigma\right) \ln(T\tau)$$

for 2D,

$$\delta\sigma_1 = \frac{e^2}{\hbar} \frac{1}{4\pi^2} \frac{1.3}{\sqrt{2}} \left(\frac{4}{3} - \frac{3}{2} \tilde{F}_\sigma\right) \sqrt{T/D}$$

for 3D,

FIG. 14. Diagrams for the correction to conductivity.

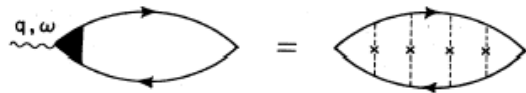


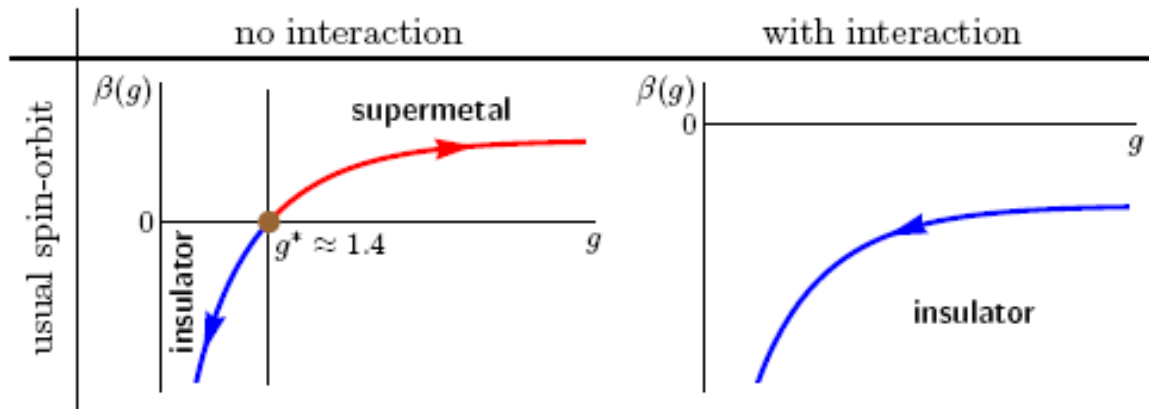
FIG. 10. Diagram for the polarization function $\Pi(q, \omega)$.

$$\begin{aligned} \Pi(q, \omega) &= i \int_0^\infty dt dx \langle [\rho(\mathbf{x}, t), \rho(0, 0)] \rangle e^{-i\mathbf{q} \cdot \mathbf{x}} e^{i\omega t} \\ &= \frac{dn}{d\mu} \frac{Dq^2}{-i\omega + Dq^2} \end{aligned}$$

$g(T)$: Full RG with AA corrections

$$\beta(g) = -1/g - 1/g \quad \text{for potential scattering } (g \gg 1)$$

$$\beta(g) = +1/2g - 1/g \quad \text{for Spin-Orbital scattering } (g \gg 1)$$



Metal-Insulator Transition in Disordered Two-Dimensional Electron Systems.

Phys. Rev. Lett. **88**, 016802 (2002).

Science (2005)

Alexander Punnoose,^{1*} Alexander M Finkel'stein²

$$\frac{d \ln \rho}{d \xi} = \rho \left[n_v + 1 - (4n_v^2 - 1) \left(\frac{1 + \gamma_2}{\gamma_2} \ln(1 + \gamma_2) - 1 \right) \right],$$

$$\frac{d \gamma_2}{d \xi} = \rho \frac{(1 + \gamma_2)^2}{2},$$

Anti-localizing effect
of interactions at
large n_v

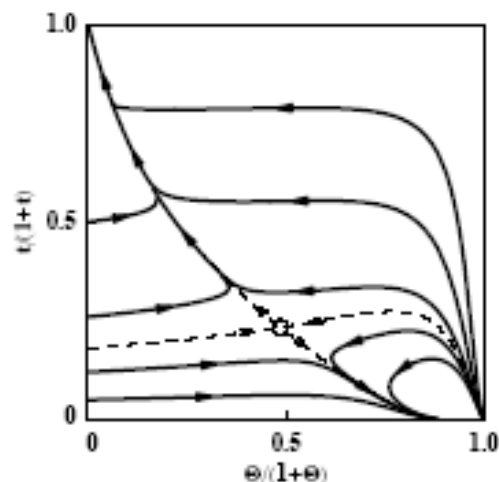


Figure 1: The disorder-interaction, t - Θ , flow diagram of the 2D electron gas obtained by solving Eqs. (4) and (5) with the Cooper channel included ($\alpha = 1$). Arrows indicate the direction of the flow as the temperature is lowered. The circle denotes the QCP of the MIT, and the dashed lines show the separatrices.

Interaction-induced criticality in \mathbb{Z}_2 topological insulators

P. M. Ostrovsky,^{1,2} I. V. Gornyi,^{1,3} and A. D. Mirlin^{1,4,5}

arXiv:0910.1338

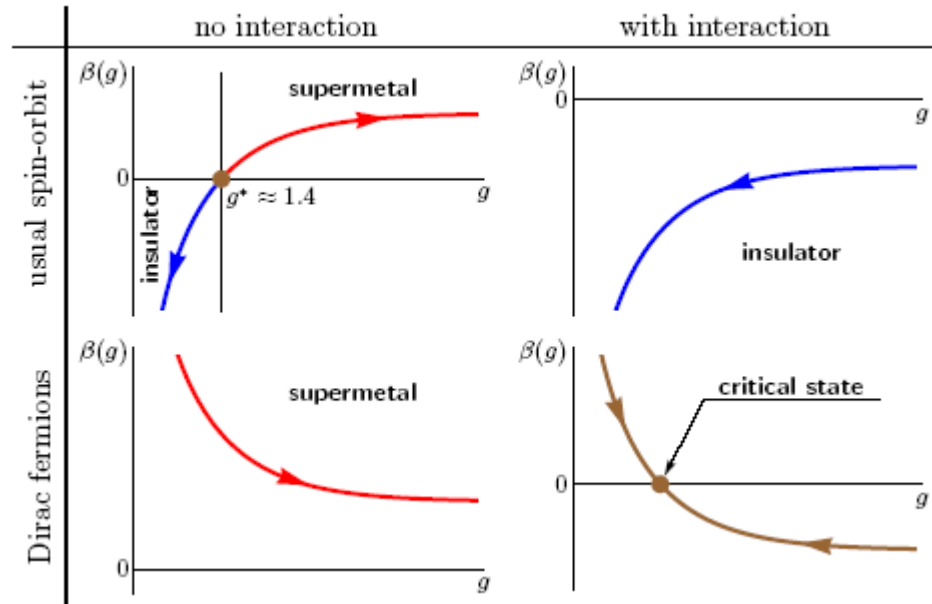
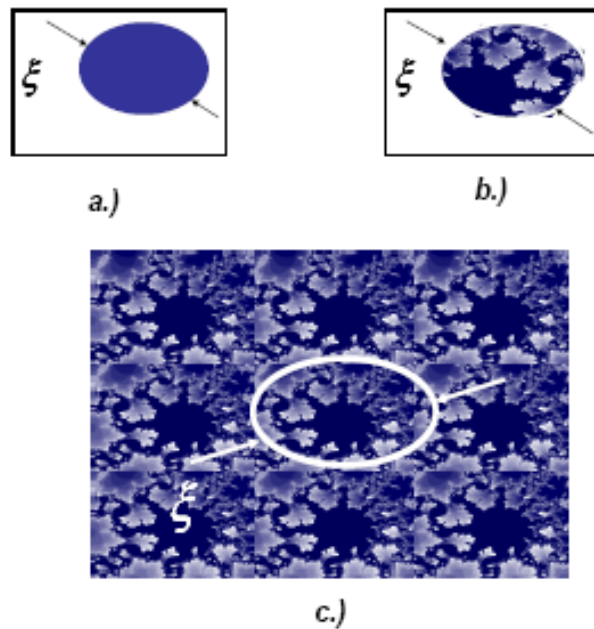


FIG. 1: Schematic scaling functions for the conductivity of 2D disordered systems of symplectic symmetry class. The plotted beta functions $\beta(g) = dg/d \ln L$ determine the flow of the dimensionless conductivity g with increasing system size L (as indicated by the arrows). The upper two panels show the beta functions for ordinary spin-orbit systems which are not topologically protected (left: no interaction; right: Coulomb interaction included). The lower two panels demonstrate the scaling for topologically protected Dirac fermions (left: no interaction; right: Coulomb interaction included).

Fractality of critical wavefunctions in 3D

Anderson Transitions [F. Evers](#), [A.D. Mirlin](#)
 Rev. Mod. Phys. 80, 1355 (2008)

E. Cuevas and V. E. Kravtsov
 Phys. Rev. B **76**, 235119 (2007)



$$P_q(E) = \rho^{-1} \sum_n \sum_{\mathbf{r}} \langle |\Psi_n(\mathbf{r})|^{2q} \delta(E - E_n) \rangle.$$

$$P_q \propto N^{-(q-1)d_q/d},$$

IPR:

$$C(\omega) = K(\omega) / \hat{R}(\omega).$$

$$K(\omega) = \int d\mathbf{r} \sum_{i,j} \langle |\Psi_i(\mathbf{r})|^2 |\Psi_j(\mathbf{r})|^2 \delta(E_i - E_j - \omega) \rangle.$$

$$R(\omega) = \sum_{i,j} \langle \delta(E_i - E_j - \omega) \rangle$$

FIG. 2: 2D cartoon of a) conventional localized state; b) localized state in a multifractal insulator; c) extended state in a multifractal metal. The darker regions correspond to higher eigenfunction amplitude. The localization/correlation radius ξ is shown in each case.

Critical eigenstates: 3D mobility edge

$$C(\omega) = \frac{1}{N} \left(\frac{E_0}{\omega} \right)^\mu, \quad \delta < \omega < E_0, \quad \mu = 1 - \frac{d_2}{d},$$

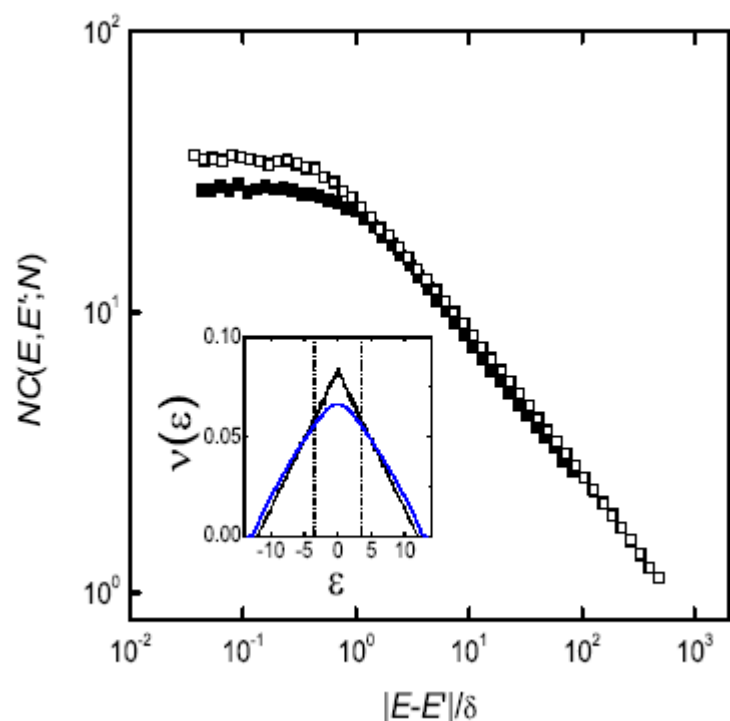


FIG. 5: Two-eigenfunction correlation function for the 3D Anderson model (orthogonal symmetry class) with a triangular distribution of random on-site energies (solid symbols) and

$$d_2/d = 0.48$$

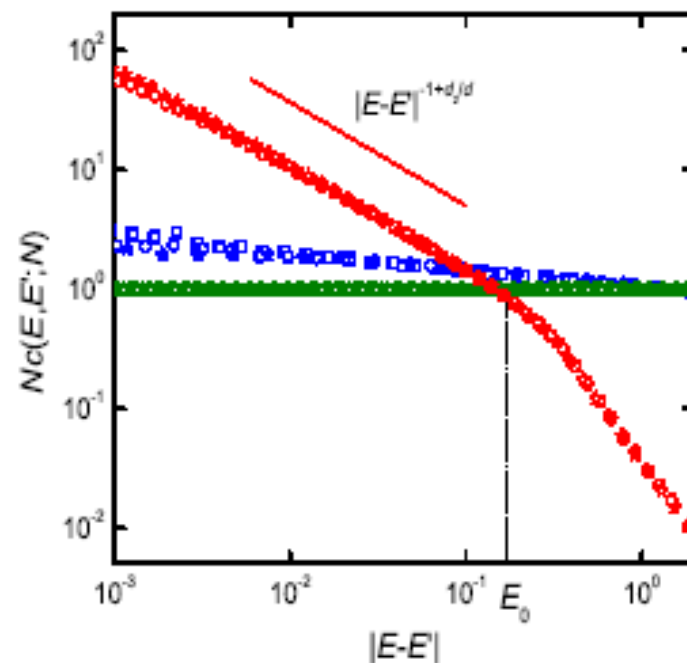


FIG. 1: Critical enhancement of eigenfunction correlation. Results of exact diagonalization of the critical PLBRM at $b = 0.1$, the banded random matrices with $B=5$, and Wigner-Dyson RM are shown in red, blue and green, respectively, and are represented by squares ($N=200$), circles ($N=1000$) and stars ($N=2000$).

Wavefunction's correlations in insulating band

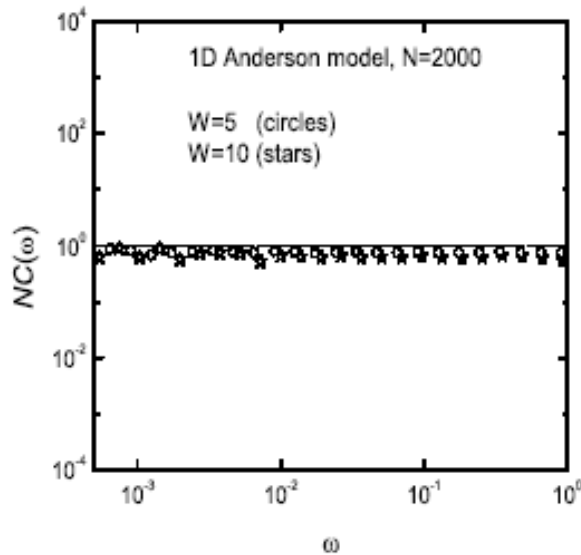


FIG. 8: Eigenfunction correlation in the 1D Anderson insulator with rectangular distribution of on-site energies and periodic boundary conditions. The disorder strength is $W = 5$ (circles), $W = 10$ (stars). The inverse participation ratio is equal to 0.23 and 0.46, respectively.

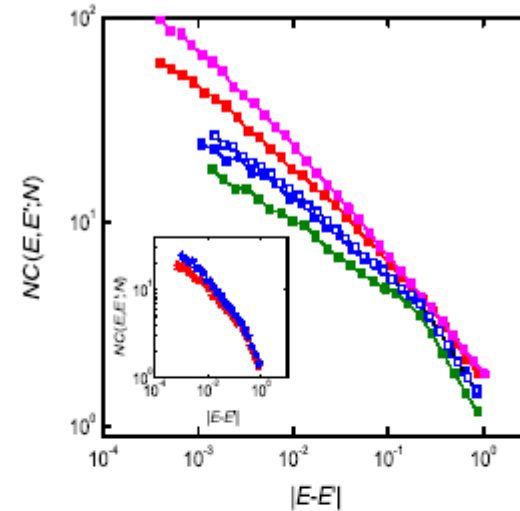


FIG. 9: Eigenfunction correlation in the 3D Anderson insulator with rectangular distribution of on-site energies and periodic boundary conditions. The disorder strength is $W = 80$ (green), $W = 60$ (blue), $W = 40$ (red), $W = 30$ (purple). The system size is $L = 20$ for filled symbols and $L = 8$ for open symbols. The inverse participation ratio for the four insulating systems is $P_2 = 0.72, 0.63, 0.44, 0.28$ which corresponds to $\xi = 1.0, 1.1, 1.2, 1.4$ according to $\xi = (9/4\pi P_2)^{1/3}$. The change of the slope occurs at $|E - E'| = \delta_\xi$. The slope for larger energy separations $|E - E'| > \delta_\xi$ progressively increases with increasing W remaining smaller than 1. The insert shows the result for $W = 60, L = 20$ for the periodic (upper blue curve) and the hard wall (lower red curve) boundary conditions.

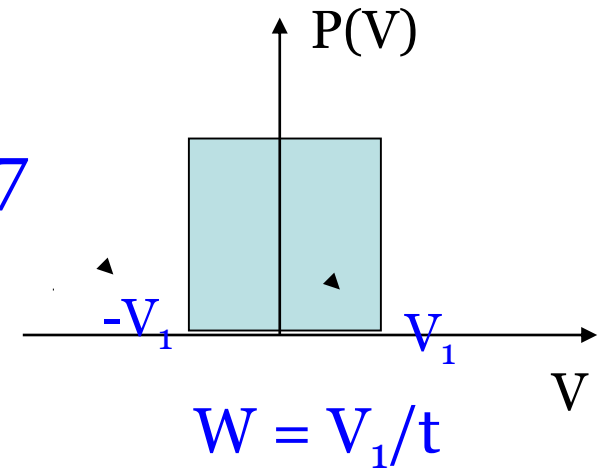
2D v/s 3D: qualitative difference

- 2D weak localization:

fractality is weak, $1-d_2/d \sim 1/g \ll 1$

- 3D critical point:

strong fractal effects, $1-d_2/d = 0.57$



3D Anderson model (“box” distribution): $W_c=16.5$
but simple diffusive metal is realized at $W < 2-3$ only



FIG. 7: A cartoon of stratification of the coordinate space: different non-intersecting supports shown by different colours. Each support corresponds to a shell of states occupying this support and thus strongly overlapping; states belonging to different shells do not overlap. The stratification of space explains both strong correlations of states at energy separation ω smaller than the single-shell bandwidth E_0 and mutual avoiding of eigenstates for $\omega > E_0$.

Anderson localization Anderson (1957)

A non-interacting electron in a random potential may be localized.

Gang of four (1979): scaling theory

Weak localization P.A. Lee, H. Fukuyama, A. Larkin, S. Hikami,

well-understood area in condensed-matter physics

Unsolved problems:

Theoretical description of critical points

Scaling theory for critical phenomena in disordered systems